Electronic Supplementary Material (ESI) for Nanoscale.

Tandem Fabrication of Upconversion Nanocomposites Enabled by Confined Protons

Xiumei Chen,[a] Jinyu Wan,[a] Minmin Wei,[a] Zhengyu Xia,[a] Jie Zhou,[a] Min Lu,[a] Ze Yuan,*[a] Ling Huang[b] and Xiaoji Xie*[a]

[a] *School of Flexible Electronics (Future Technologies) & Institute of Advanced Materials (IAM), Nanjing Tech University (NanjingTech), 30 South Puzhu Road, Nanjing 211816, China*

[b] *State Key Laboratory of Chemistry and Utilization of Carbon Based Energy Resources, College of Chemistry, Xinjiang University, Urumqi 830046, China*

** Email: iamzyuan@njtech.edu.cn; iamxjxie@njtech.edu.cn*

1. Experimental Section

1.1 Materials

Tetrakis(4-carboxyphenyl) porphyrin (TCPP, >97%) was purchased from Chemsoon Co. Ltd. Poly(acrylic acid) ($(C_3H_4O_2)_n$, M.W. ~2000) was purchased from Macklin. Cesium carbonate (Cs_2CO_3, 99.9%), polyvinyl pyrrolidone (PVP, M.W. ~55000), and octadecylamine (≥99%) were obtained from Sigma-Aldrich. 1,3,5-benzenetricarboxylic acid (BTC, 98.0%) was purchased from Alfa Aesar. N-methylformamide (NMF, 99%) was purchased from Energy Chemical. Calcium nitrate tetrahydrate ($Ca(NO_3)_2·4H_2O$, ≥99%), sodium fluoride (NaF, ≥99%), trisodium phosphate (Na_3PO_4, ≥98%), bismuth chloride ($BiCl_3$, ≥98%), acetic acid (CH_3COOH, ≥99.5%), lithium hydroxide (LiOH, 99%), sodium chloride (NaCl, >99.8%), potassium chloride (KCl, >99.8%), lithium chloride (LiCl, ≥95%), magnesium chloride hexahydrate ($MgCl_2·6H_2O$, ≥98%), calcium chloride dihydrate ($CaCl_2·2H_2O$, >99%), barium chloride dihydrate ($BaCl_2·2H_2O$, ≥99.5%), copper(II) chloride dihydrate ($CuCl_2·2H_2O$, ≥99%), zinc chloride ($ZnCl_2$, >98%), nickel(II) chloride hexahydrate ($NiCl_2·6H_2O$, ≥98%), copper acetate monohydrate ($Cu(CH_3CO_2)_2·H_2O$, 98~102%), copper nitrate trihydrate ($Cu(NO_3)_2·3H_2O$, 99%~102%), copper sulfate pentahydrate ($CuSO_4·5H_2O$, ≥99%), ferric nitrate nonahydrate ($Fe(NO_3)_3·9H_2O$, ≥98.5%), ferric sulfate hydrate ($Fe_2(SO_4)_3·9H_2O$, AR), ferric trichloride hexahydrate ($FeCl_3·6H_2O$, ≥99%), stannic chloride pentahydrate ($SnCl_4·5H_2O$, ≥99%), aluminum nitrate nonahydrate ($Al(NO_3)_3·9H_2O$, ≥99%), gallium nitrate hydrate ($Ga(NO_3)_3·xH_2O$, 99%), citric acid monohydrate ($C_6H_8O_7·H_2O$, >99%), and all the other chemicals were received from Sinopharm Chemical Reagent Beijing Co., Ltd. All chemicals were used as received unless otherwise noted.

1.2 Synthesis of $NaGdF_4$:Yb/Tm (49/1 mol%) nanoparticles

Typically, an aqueous solution (2 mL) containing $Gd(CH_3COO)_3$ (0.2 mmol), $Yb(CH_3COO)_3$ (0.196 mol), and $Tm(CH_3COO)_3$ (0.004 mmol) was mixed with oleic acid (4 mL) and 1-octadecene (ODE) (6 mL) in a 50 mL two-neck round-bottom flask. The mixture was heated at 150 °C for 1 h to remove water, followed by cooling to 50 °C. After the mixture was mixed with a methanol solution (5.3 mL) containing NH_4F (1.32 mmol) and NaOH (1 mmol), the reaction mixture was stirred at 50 °C for 2 h and then heated to 100 °C in order to remove the

low boiling solvent. Subsequently, the mixture was heated to 280 ºC under a nitrogen atmosphere and kept for 1.5 h before cooling to room temperature. The resulting $NaGdF_4$:Yb/Tm nanoparticles were precipitated by ethanol, collected by centrifugation, and washed with ethanol. Finally, the nanoparticles were redispersed in cyclohexane (4 mL) for further use.

1.3 Synthesis of $NaGdF_4$:Yb/Tm (49/1 mol%)@$NaGdF_4$ and $NaGdF_4$:Yb/Tm (49/1 mol%)@$NaGdF_4$:Tb (15 mol%) core-shell nanoparticles

To obtain $NaGdF_4$:Yb/Tm (49/1 mol%)@$NaGdF_4$ core-shell nanoparticles, a mixture, containing an aqueous solution (1 mL) of $Gd(CH_3COO)_3$ (0.2 mmol), oleic acid (4 mL), and ODE (6 mL), was firstly heated at 150 ºC in a two-neck round-bottom flask (50 mL) for 1 h to form a reaction precursor for shell coating. After the mixture was cooled to 50 ºC, the as-synthesized $NaGdF_4$:Yb/Tm(49/1 mol%) core nanoparticles (in cyclohexane, 4 mL), along with a methanol solution (2.7 mL) of NH_4F (0.68 mmol) and NaOH (0.5 mmol), were added, and the resulting mixture was kept at 50 ºC for 2 h under continuous stirring. Subsequently, the mixture was heated at 100 ºC to remove the low boiling solvent and then heated at 280 ºC for 1.5 h under a nitrogen atmosphere. After the reaction mixture was cooled to room temperature, the $NaGdF_4$:Yb/Tm@$NaGdF_4$ core-shell nanoparticles were precipitated by ethanol, collected by centrifugation, washed with ethanol, and redispersed in cyclohexane for further use. To coat the $NaGdF_4$:Yb/Tm (49/1 mol%) nanoparticles with a $NaGdF_4$:Tb (15 mol%) shell, the same procedures as that for preparing $NaGdF_4$:Yb/Tm (49/1 mol%)@$NaGdF_4$ core-shell upconversion nanoparticles were used. Specifically, $Gd(CH_3COO)_3$ (0.17 mmol) and $Tb(CH_3COO)_3$ (0.03 mmol) were used as the rare earth source during the preparation of shell precursor.

1.4 Synthesis of $LiYF_4$:Yb/Tm (20/1 mol%) nanoparticles

Typically, an aqueous solution containing $Y(CH_3COO)_3$ (0.32 mmol), $Yb(CH_3COO)_3$ (0.08 mmol), and $Tm(CH_3COO)_3$ (0.004 mmol), was mixed with oleic acid (3 mL) in a two-neck round-bottom flask (50 mL). The mixture was then heated at 130 ºC for 0.5 h before the addition of ODE (7 mL). Subsequently, the resulting solution was heated at 150 ºC for another 0.5 h,

cooled to room temperature, and mixed with a methanol solution (6 mL) containing NH_4F (1.6 mmol) and LiOH (1 mmol). The obtained reaction mixture was heated at 50 ºC for 0.5 h and then heated to 100 ºC to remove the low boiling solvent. After that, the reaction mixture was heated to 290 ºC under a nitrogen atmosphere and kept for 1.5 h. After the reaction mixture was cooled to room temperature, the final products were precipitated by ethanol, collected by centrifugation, washed with ethanol for three times, and redispersed in cyclohexane for further use.

1.5 Synthesis of $NaLaF_4$ nanoparticles

Typically, an aqueous solution, containing $La(CH_3COO)_3$ (0.4 mmol), CH_3COONa (2 mmol), and Cs_2CO_3 (0.8 mmol), was mixed with oleic acid (3 mL) and ODE (7 mL) in a 50 mL two-neck round-bottom flask. The mixture was heated at 170 ºC for 0.5 h before cooling to 45 ºC. Subsequently, a methanol solution (6 mL) containing NH_4F (2.4 mmol) was added, and the resulting mixture was stirred at 45 ºC for 2 h. After the methanol was evaporated at 110 °C, the mixture was degassed through a vacuum pump for 5 min, heated to 310 °C, and maintained at 310 °C under a nitrogen atmosphere for 1 h. The reaction mixture was then cooled to room temperature, and the final products were precipitated by ethanol, collected by centrifugation, washed with ethanol and methanol for three times, and redispersed in cyclohexane for further use.

1.6 Synthesis of F-doped hydroxyapatite (FHAP) spindle nanomaterials

FHAP spindle nanomaterials were synthesized according to a reported method.[1] Generally, in a Teflon-lined autoclave, ethanol (16 mL) was mixed with octadecylamine (0.5 g) and oleic acid (4 mL) by stirring. Then, an aqueous solution (7 mL) containing $Ca(NO_3)_2{\cdot}4H_2O$ (322 mg) and $Eu(NO_3)_3{\cdot}6H_2O$ (43.7 mg) was added. Subsequently, an aqueous solution (7 mL) dissolving NaF (11.8 mg) and Na_3PO_4 (16.3 mg) was dripped into the mixture. The mixture was agitated for 5 min, then transferred into the autoclave, and subsequently heated at 150 °C for 12 h. The obtained FHAP nanomaterials were collected by centrifugation, and washed with a mixture of cyclohexane and ethanol for three times. Finally, the as-synthesized nanomaterials were redispersed in cyclohexane for further use.

1.7 Synthesis of EuOOH nanowires

EuOOH nanowires were synthesized via a modified method according to the previous report.[2] Generally, 1.2 g of $EuCl_3$ was first dissolved in water (1.5 mL) under stirring and then mixed with ethanol (18 mL). The solution was added into a mixture of oleic acid (3 mL) and oleylamine (6 mL) in a 40 mL Teflon-lined autoclave. After the resulting mixture was vigorously stirred for 15 min, the autoclave was sealed and heated at 160 °C for 8 h, and then cooled to room temperature. The products were collected by centrifugation, and washed with a mixture of cyclohexane and ethanol for three times. Finally, the as-synthesized nanowires were redispersed in cyclohexane for further use.

1.8 Synthesis of Bi_2S_3 nanorods

Bi_2S_3 nanorods were synthesized according to a reported method.[3] Typically, a mixture of $BiCl_3$ (1 g) and oleylamine (4.2 mL) was first added to a 25 mL three-necked flask. The mixture was then stirred and heated to 170 °C under a N_2 atmosphere for 40 min. Subsequently, 10.4 mL of oleylamine containing sulfur (0.5 g) was swiftly injected into the flask. The color of the mixture turned to red brown immediately after injection, indicating the formation of Bi_2S_3 seeds. The Bi_2S_3 seeds were then allowed to grow at 130 °C for 1 h before the reaction was quenched with cold hexane. The products were collected by centrifugation, washed with ethanol for three times, and redispersed in cyclohexane for further use.

1.9 Synthesis of Fe_3O_4 nanoparticles

Fe_3O_4 nanoparticles were synthesized according to a reported method.[4] Firstly, ferric oleate was synthesized by reacting $FeCl_3$ with sodium oleate. Typically, 3.65 g of sodium oleate was dissolved in a mixture of ethanol (8 mL) and hexane (14 mL) by stirring. Then, an aqueous solution (6 mL) containing anhydrous $FeCl_3$ (0.65 g) was added. The resulting two-phase mixture was heated to 70 ºC and vigorously stirred for 4 h. After the reaction mixture was cooled to room temperature, the mixture was washed three times with distilled water and hexane, and the organic layer was collected using a separatory funnel. Ferric oleate was obtained by evaporating the solvent of organic layer at 80 °C overnight. The resulting ferric oleate was

dissolved in a mixture of oleic acid (0.624 mL) and 1-octadecene (25 mL) at room temperature, degassed with N_2 for 0.5 h, and heated at 320 °C for 0.5 h. Upon the mixture was cooled to room temperature, the products were collected by centrifugation, and washed with a mixture of cyclohexane and ethanol for three times. Finally, the as-synthesized nanoparticles were redispersed in cyclohexane for further use.

1.10 Transferring ligand-capped nanomaterials to the non-aqueous polar solvent by confined protons

Generally, transferring different ligand-capped nanomaterials to the non-aqueous polar solvent follows similar procedures. Using DMF as a representative non-aqueous polar solvent, in a typical experiment, a DMF solution (0.8 mL) containing $Al(NO_3)_3 \cdot 9H_2O$ (0.02 mmol) was mixed with a cyclohexane solution (0.8 mL) containing ligand-capped nanomaterials (2.5 mg) in a vial. The mixture was then shaken for ~10 s before layering. After that, the DMF layer was collected for further use. The same procedures were used when other metal salts were applied as proton generators. When inorganic acids were used as proton generators, inorganic acids in high concentrations were added to DMF, yielding a DMF solution of inorganic acid with a concentration of 0.1 M. Notably, to transfer the as-synthesized Bi_2S_3 nanomaterials to the non-aqueous polar solvent, N-methylformamide was employed, and the transfer was initiated by vigorously stirring for 2 min.

The resulting ligand-free nanomaterials in DMF were collected by centrifugation with a certain speed. The speed and duration of centrifugation were selected according to the type of nanomaterials. Generally, a speed of 16000 rpm and a duration of 15 min were used for the collection. The collected nanomaterials were washed with a mixture of DMF and ethanol for two times, and redispersed in a polar solvent, such as DMF, for further use.

On a separate note, using the as-synthesized UCNPs as the representative, we found that at least ~0.002 mmol of metal salts (proton generators) was required to obtain ligand-free nanomaterials under our reaction conditions. Taking $ZrCl_4$ as an example, when $ZrCl_4$ with a small amount of 0.002 mmol (dissolved in 0.8 mL DMF) was reacted with pristine UCNPs (2.5 mg, dispersed in 0.8 mL cyclohexane) by shaking, UCNPs can be thoroughly brought to DMF after reaction (Fig. E1), indicating the nearly complete removal of oleate from UCNPs.

Differently, when 0.001 mmol of $ZrCl_4$ was used under the same conditions, only some UCNPs were brought to DMF (Fig. E1b), and many UCNPs remained in cyclohexane (Fig. E1b), revealing the incomplete removal of ligands.

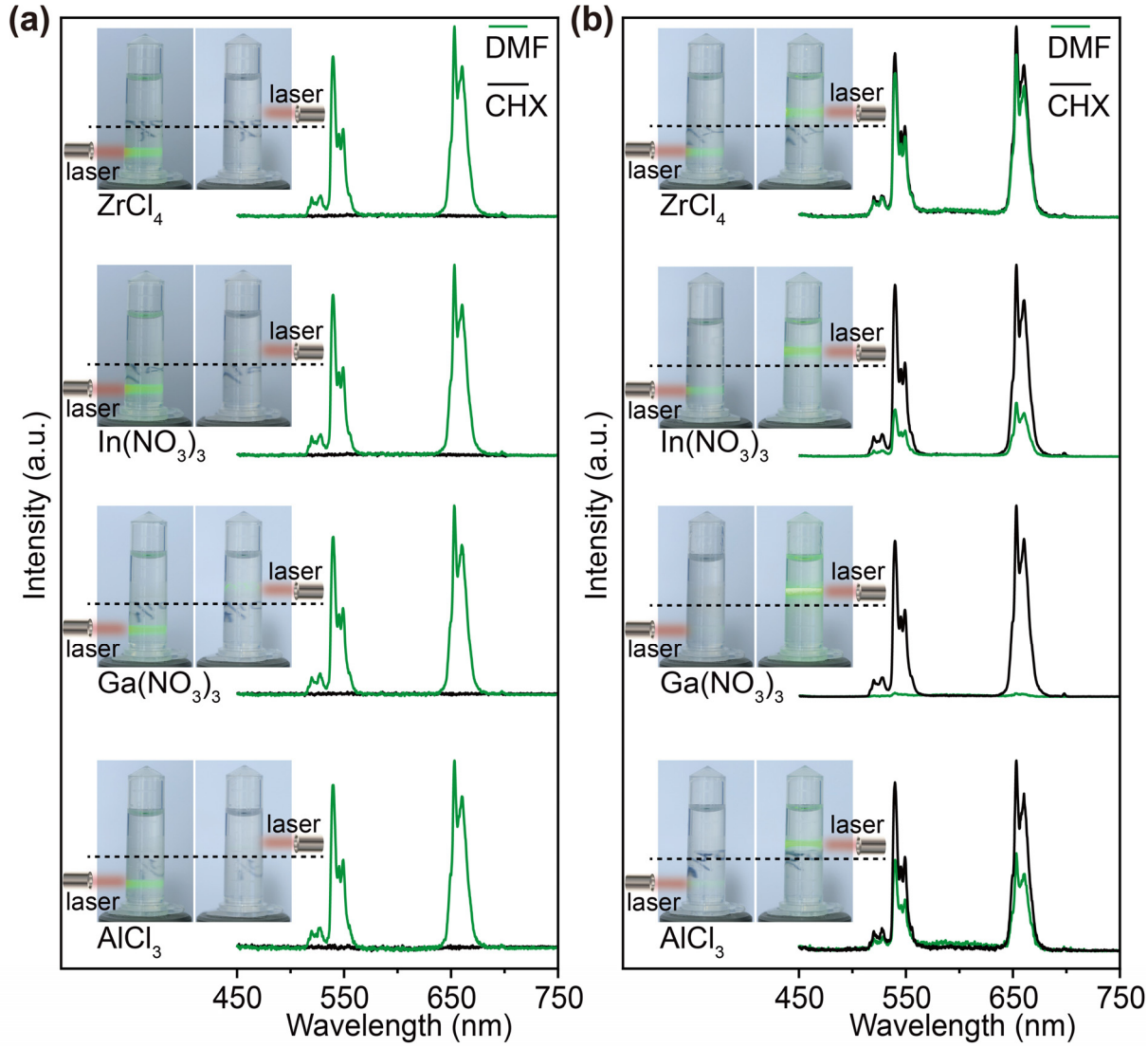

Figure E1. Upconversion spectra of the DMF and cyclohexane (CHX) layer after ligand-stripping reaction conducted by employing (a) 0.002 and (b) 0.001 mmol of proton generators ($ZrCl_4$, $In(NO_3)_3$, $Ga(NO_3)_3$, and $AlCl_3$), respectively. Insets are corresponding photos of the reaction mixtures in tubes after the reaction, in which the position of liquid-liquid interfaces are indicated by dashed lines. The tubes are irradiated by a 980 nm laser to check emission spectra of two layers, and the green lines in the photos are the upconversion luminescence from UCNPs.

A similar minimum amount was determined for other metal salts (proton generators), such as $In(NO_3)_3$, $Ga(NO_3)_3$, and $AlCl_3$ (Fig. E1), using the same method. It is worth noting that when the amount (or concentration) of employed proton generators is small, repeated shaking and layering can be required to completely remove ligands. For example, 0.002 mmol of $ZrCl_4$ (dissolved in 0.8 mL DMF) needs shaking and layering for ~5 times to completely remove ligands. To ensure the fast and efficient removal of ligands, we reason that 0.002 mmol should be the required minimum amount of metal salts (proton generators) under our conditions.

Regarding the molar amount of generated H^+ under our conditions, we found that the molar amount should be ~0.002 mmol in the typical ligand removal reaction. Specifically, according to the thermogravimetric analysis (Fig. 3e), 2.5 mg of pristine UCNPs can have ~0.002 mmol of oleate on their surface.

The ligand removal process can be generally expressed by the following chemical reactions (using Zr salts as an example):

$$NaOA + H_2O + Zr^{4+} \rightleftharpoons Zr(OH)^{3+} + HOA + Na^+$$

$$Ln(OA)_3 + 3H_2O + 3Zr^{4+} \rightleftharpoons 3Zr(OH)^{3+} + 3HOA + Ln^{3+}$$

In these reactions, OA represents oleate. NaOA and $Ln(OA)_3$ represent the coordination forms of oleate ligands with the exposed Na^+ and Ln^{3+} on UCNPs, respectively. According to these reactions, we can conclude that the amount of generated H^+ should be equal to the amount of oleate capped on UCNPs. As a result, proton generators should generate ~0.002 mmol of H^+ to remove all the oleate.

To gain more insights into the proton generation process, we further detected the proton concentration in our reaction system by a spectroscopic method. Specifically, $NaGdF_4$:Yb/Tm (49/1 mol%)@$NaGdF_4$-terephthalic acid-Tb^{3+} ($NaGdF_4$-BDC-Tb^{3+}) nanomaterials were synthesized according to our previous study,[5] and then employed as the optical proton probe. In should be mentioned that in our previous study, we showed that protons can detach BDC from the $NaGdF_4$-BDC-Tb^{3+}, thereby blocking the energy transfer from $NaGdF_4$ to Tb^{3+}, which bleaches the upconversion emission of Tb^{3+} at ~543 nm.[5] Thus, the emission of Tb^{3+} at ~543 nm can be used to determine the amount of protons.

The curve of emission intensity at ~543 nm in logarithmic scale (Log I_{543}) against the proton concentration was plotted based on the upconversion emission spectra of a $NaGdF_4$-

BDC-Tb^{3+} probe solution (1.25 mg probe in 1 mL DMF) after the gradual addition of HCl (10 μM in DMF) (Fig. E2). We observed a nearly linear dependence of Log I_{543} on the proton concentration, when the proton concentration varied from 0.06 to 0.084 μM (Fig. E2b). These results enable us to use $NaGdF_4$-BDC-Tb^{3+} to detect the proton concentration in the DMF solution of $ZrCl_4$.

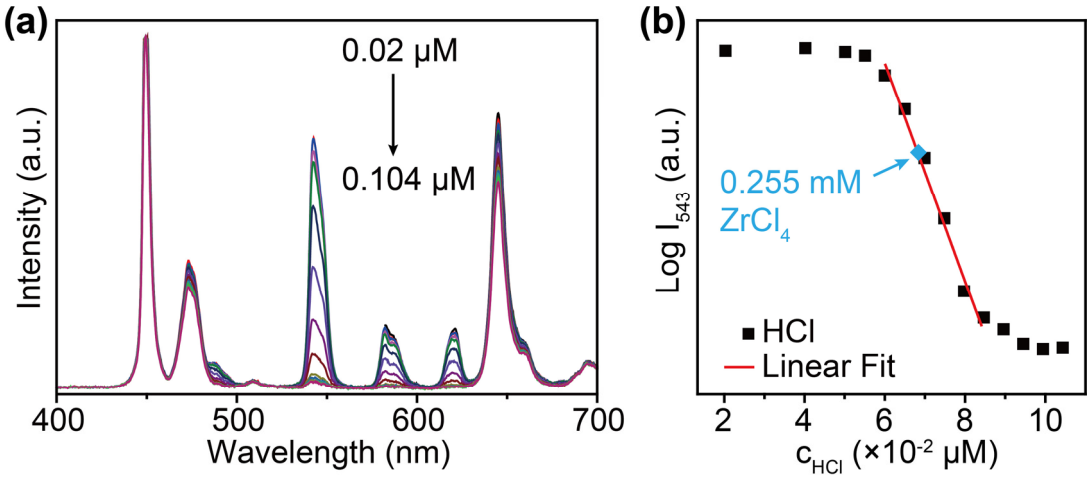

Figure E2. (a) Upconversion spectra of $NaGdF_4$-BDC-Tb^{3+} probe dispersed in DMF against the concentration of HCl. (b) Corresponding Log I_{543} as a function of the HCl concentration. The Log I_{543} value of probe in the presence of 0.255 mM $ZrCl_4$ is indicated by the blue rhomb. Note that the emission intensity was obtained by integrating the Tb^{3+} emission from 525 to 564 nm.

To determine the proton concentration in the DMF solution of $ZrCl_4$ under our conditions, the probe was added to the DMF solution containing 0.255 mM of $ZrCl_4$. Then, the emission spectrum of the mixture was recorded, and corresponding Log I_{543} was calculated. On the basis of the obtained Log I_{543} value and the calculating curve shown in Fig. E2b, we calculated that the proton concentration in the DMF solution of 0.255 mM $ZrCl_4$ was 0.068 μM.

Typically, the hydrolysis of Zr^{4+} undergoes the following reaction:

$$Zr^{4+} + H_2O \rightleftharpoons Zr(OH)^{3+} + H^+$$

Accordingly, we can obtain:

$$K_h(Zr^{4+}) = \frac{[Zr(OH)^{3+}][H^+]}{[Zr^{4+}]} \qquad \text{(Eq. 1)}$$

where K_h (Zr^{4+}) is the first order hydrolysis constant of Zr^{4+}, and [$Zr(OH)^{3+}$], [H^+], as well as [Zr^{4+}] are concentrations of $Zr(OH)^{3+}$, proton, and Zr^{4+}, respectively. According to Eq. 1 and the determined [H^+] (0.068 μM) in the DMF solution of $ZrCl_4$ (0.255 mM), the calculated K_h (Zr^{4+}) is 1.81×10^{-5} in DMF. Thus, under our reaction conditions, we can estimate that the proton concentration is ~21.3 μM when 0.02 mmol (the amount we used) of $ZrCl_4$ is used, and ~6.7 μM when 0.002 mmol (the minimum amount needed) of $ZrCl_4$ is used. It should be noted that the high-order hydrolysis of metal ions is weak, and thus can be ignored for simplification.

1.11 Stripping native ligands of nanomaterials by the HCl washing method

Typically, ligand-capped nanomaterials (~10 mg) were first dispersed in ethanol (0.75 mL) by sonication and then mixed with an aqueous solution of HCl (0.75 mL, 1 M). The resulting mixture was sonicated for 1 min, and the nanoparticles were then collected by centrifugation (16,000 rpm, 15 min). The acid treatment was repeated two times to ensure the complete removal of ligands. The ligand-free nanomaterials were further washed with ethanol and redispersed in a polar solvent for further use. Notably, the concentration of HCl can be adjusted according to the type of nanomaterials.

1.12 Synthesis of UCNPs-Fe_3O_4-MOF nanocomposite

Typically, a DMF solution (2 mL), containing $ZrCl_4$ (2.1 mg) and 1,4-benzenedicarboxylic acid (1.4 mg), was first mixed with acetic acid (0.24 mL). Then, a cyclohexane solution (1 mL), containing oleate ligand-capped $NaYF_4$:Yb/Er (0.5 mg) and Fe_3O_4 (1 mg) nanoparticles, was added to the DMF solution, and the resulting mixture was shaken for ~10 s. After the mixture separated into two layers, the DMF layer was transferred to a vial (5 mL) and kept at 120 °C for 24 h to obtain the UCNPs-Fe_3O_4-MOF nanocomposite. Finally, the as-synthesized nanocomposites were collected by centrifugation, washed with DMF for three times, and dispersed in DMF for further use.

1.13 Synthesis of nanoparticle-MIL-100(Al) composite gel

To obtain nanoparticle-MIL-100(Al) composite gel, a DMF solution (0.5 mL), containing 1,3,5-benzenetricarboxylic acid (0.066 mmol) and $Al(NO_3)_3\cdot9H_2O$ (0.066 mmol), were mixed

with a cyclohexane (0.5 mL) solution containing ligand-capped nanoparticles (UCNPs: 4 mg or Fe_3O_4: 7 mg). The resulting mixture was shaken for ~10 s before layering. Then, the DMF layer was added to a vial (5 mL) and kept at 120 ºC in an oven for 24 h to obtain the composite gel. The composite gel was washed with DMF for two times and ethanol for one time, and finally dried at room temperature for further characterization.

1.14 Synthesis of UCNP-linker nanocomposite

Typically, a DMF solution (1.6 mL), containing a target linker (0.06 mmol) and $Al(NO_3)_3 \cdot 9H_2O$ (1.5 mg), was mixed with a cyclohexane solution (1.6 mL), containing oleate ligand-capped $NaYF_4$:Yb,Er nanoparticles (5 mg). The resulting mixture was stirred for 5 min at room temperature before it separated into two layers. The DMF layer was then added to a 5 mL vial, and then stirred at 60 ºC for 0.5 h before cooling down to room temperature. The as-synthesized nanocomposites were collected by centrifugation, washed with DMF for three times, and dispersed in DMF for further use.

1.15 Synthesis of UCNP-linker-EuOOH nanocomposite

Typically, a DMF solution (2 mL) containing 1,4-benzenedicarboxylic acid (10 mg) and $Al(NO_3)_3 \cdot 9H_2O$ (1.5 mg) was mixed with a cyclohexane solution (2 mL) containing as-synthesized EuOOH (4.5 mg) and $NaGdF_4$:Yb/Tm (49/1 mol%)@$NaGdF_4$ UCNPs (3 mg). The resulting mixture was stirred for 5 min at room temperature before layering. The DMF layer was then added to a 5 mL vial, and stirred at 60 ºC for 3 h before cooling to room temperature. The as-synthesized nanocomposites were collected by centrifugation, washed with DMF for three times, and dispersed in DMF for further use.

2. Supplementary Figures and Tables

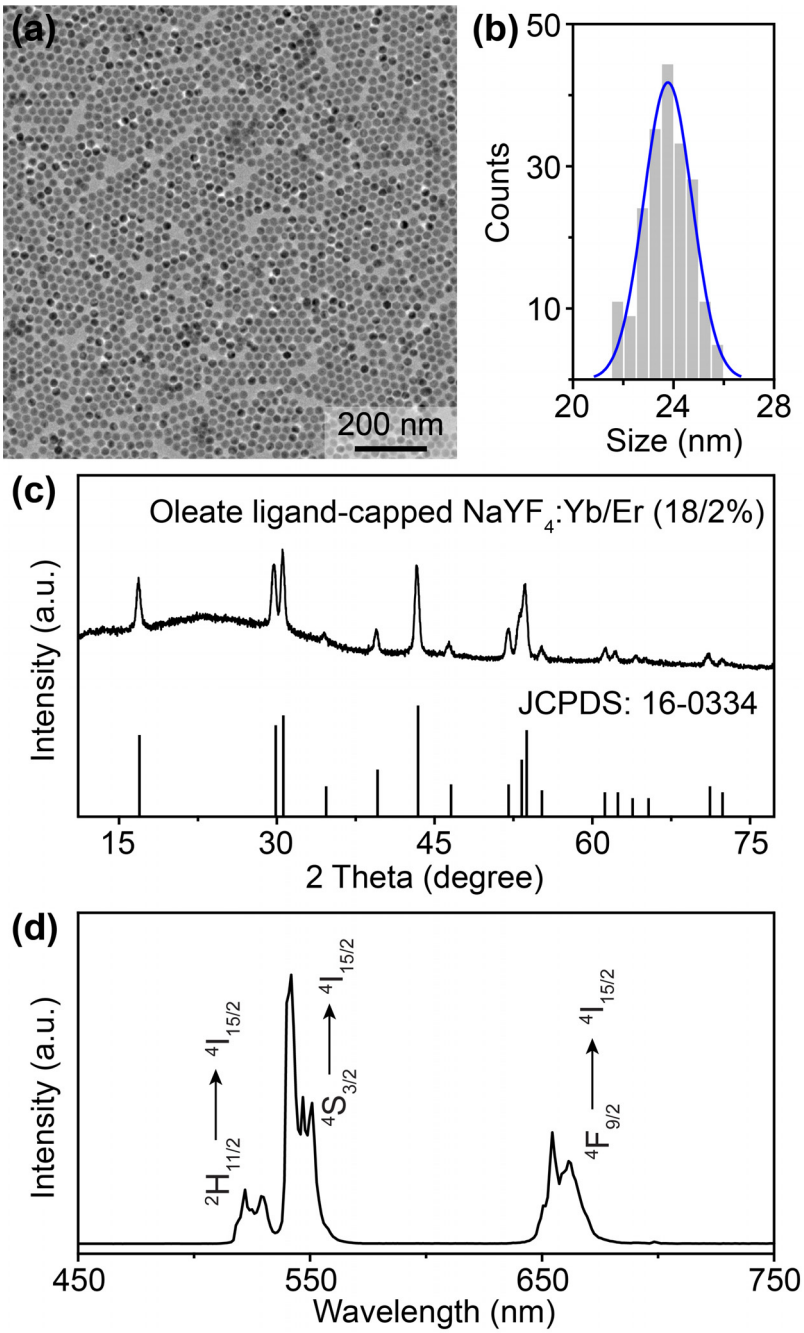

Figure S1. (a) Large scale TEM image, (b) corresponding size distribution, (c) XRD pattern, and (d) upconversion luminescence spectrum of the oleate ligand-capped hexagonal $NaYF_4$:Yb/Er (18/2 mol%) nanoparticles dispersed in cyclohexane. The diffraction pattern at the bottom of (c) is the literature reference for the hexagonal $NaYF_4$ crystal (JCPDS: 16-0334).

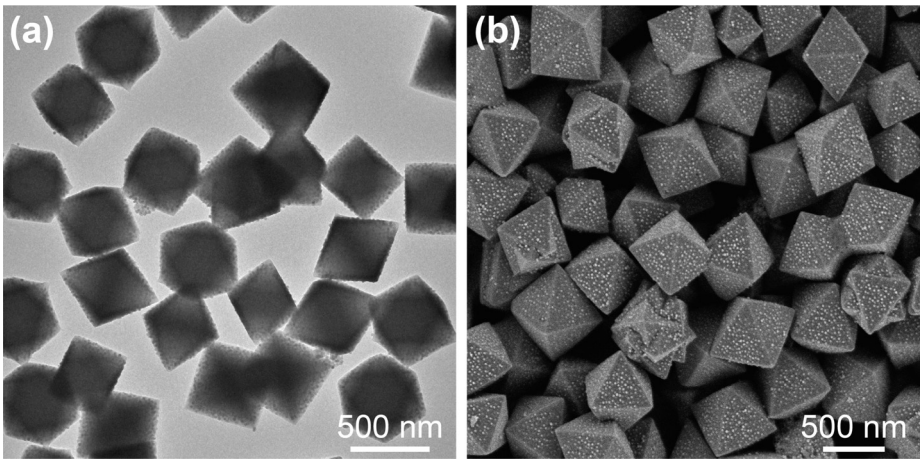

Figure S2. Large scale (a) TEM and (b) SEM images of the obtained UiO-66@UCNPs nanocomposites.

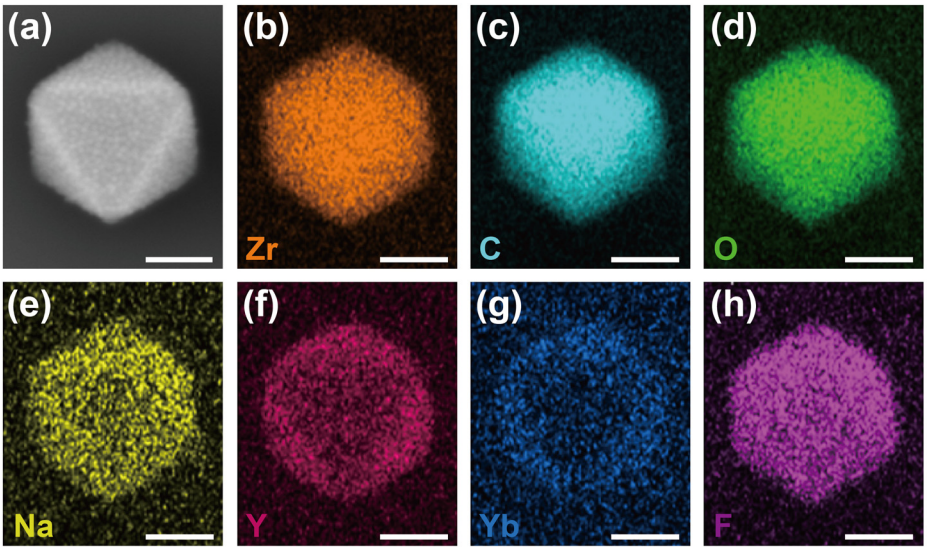

Figure S3. (a) SEM image of a randomly selected UiO-66@UCNPs nanocomposite and (b–h) corresponding elemental mapping. Scale bars are 200 nm.

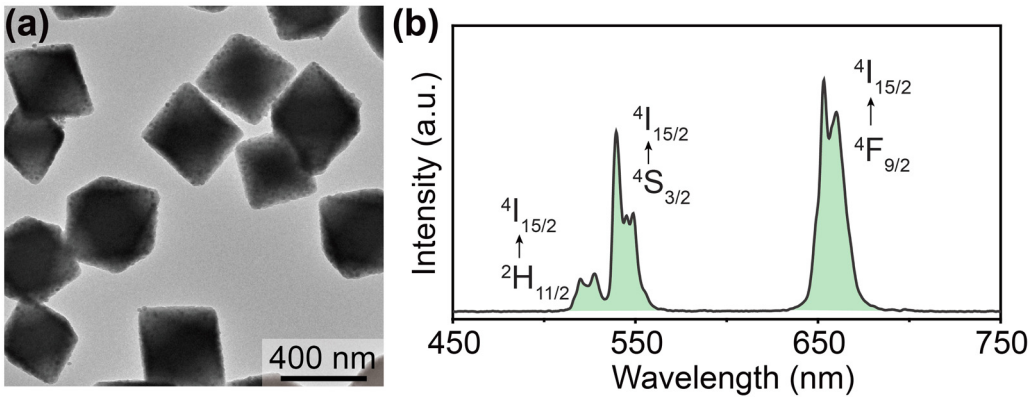

Figure S4. (a) TEM image and (b) corresponding upconversion luminescence spectrum of the UiO-66@UCNPs nanocomposites obtained by a large-scale synthesis. The nanocomposites were dispersed in DMF for measuring the spectrum.

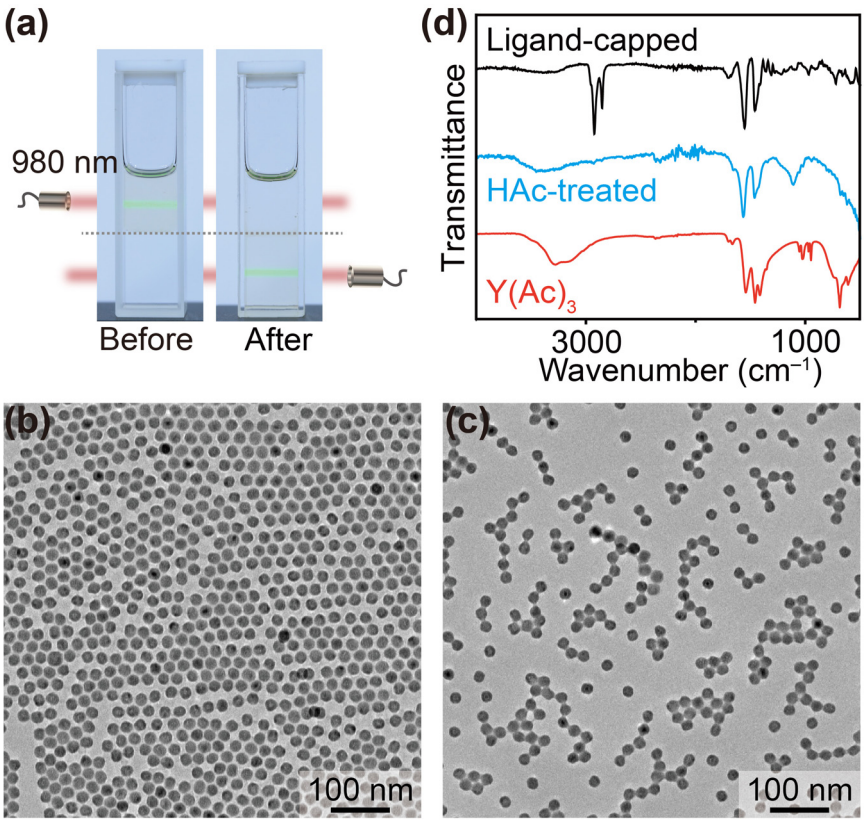

Figure S5. (a) Photos of a cuvette containing the mixture of oleate ligand-capped UCNPs in cyclohexane and acetic acid in DMF before and after a ~10 s shake. The cuvette is irradiated by a 980 nm laser to check the position of UCNPs. The dotted line indicates the position of the liquid-liquid interface, where cyclohexane stays on top and DMF stays at the bottom. (b, c) TEM images of (b) oleate ligand-capped UCNPs and (c) UCNPs collected after the acetic acid (HAc) treatment. (d) FT-IR spectra of UCNPs shown in both (b) and (c) and yttrium acetate ($Y(Ac)_3$). After the oleate ligand-capped UCNPs were treated by acetic acid, the oleate ligands were removed as indicated by the disappearance of characteristic peaks of oleate ligands (e.g., peaks at ~2924 and 2854 cm^{-1}). In the FT-IR spectrum of UCNPs collected after the acetic acid treatment, peaks at ~1568 and 1461 cm^{-1} should be due to the attachment of acetic groups on the surface of UCNPs as indicated by the FT-IR spectrum of $Y(Ac)_3$.

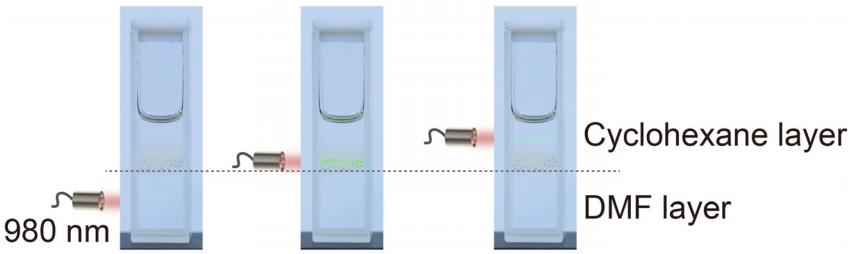

Figure S6. Photos of a cuvette containing the mixture of oleate ligand-capped UCNPs in cyclohexane and 1,4-benzenedicarboxylic acid in DMF after a ~10 s shake. The dotted line indicates the position of the liquid-liquid interface. After the treatment, UCNPs remain in cyclohexane.

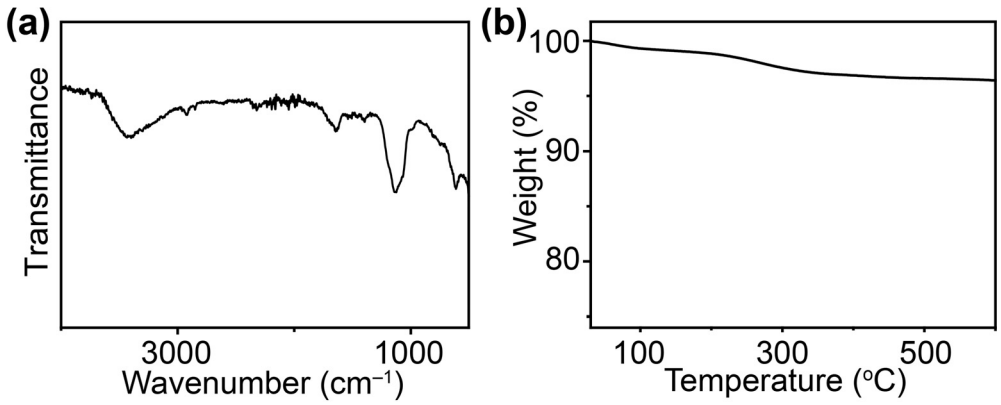

Figure S7. (a) FT-IR spectrum and (b) TG profile of ligand-free UCNPs prepared by the typical HCl acid washing method.

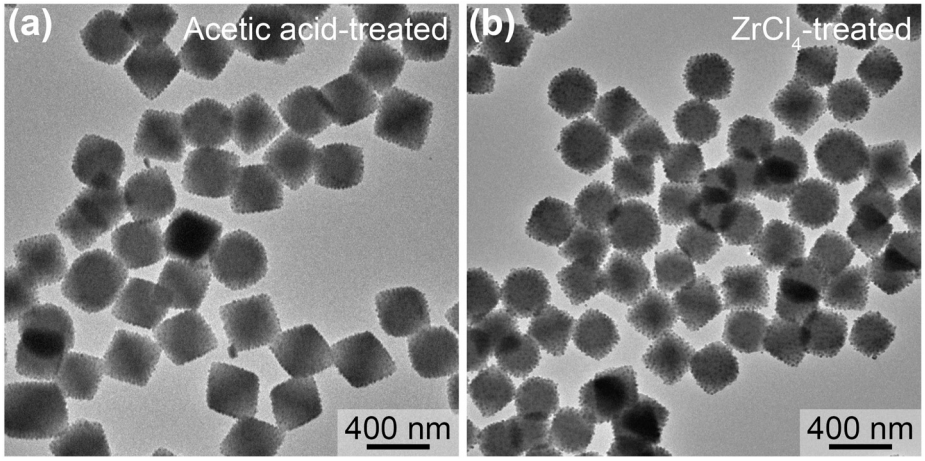

Figure S8. TEM images of UiO-66@UCNPs nanocomposites prepared by using (a) acetic acid-treated UCNPs and (b) $ZrCl_4$-treated UCNPs as the upconversion part. UCNPs were first transferred to DMF by the acetic acid or $ZrCl_4$ treatment. After that, other reaction precursors of nanocomposites were added to the DMF solution containing UCNPs for synthesizing the composite.

Table S1. pH values of the aqueous solution of different metal salts.[a]

Metal salts	pH	Metal salts	pH
$SnCl_4$	0.908	$CeCl_3$	5.390
$ZrCl_4$	0.914	$GdCl_3$	5.017
$Fe(NO_3)_3$	1.621	$EuCl_3$	5.873
$FeCl_3$	1.678	$LuCl_3$	5.229
$Fe_2(SO_4)_3$	3.843	$TmCl_3$	5.763
$C_4H_7FeO_5$	5.101	$LaCl_3$	5.673
$Ga(NO_3)_3$	2.192	$TbCl_3$	5.102
$Al_2(SO_4)_3$	2.665	$DyCl_3$	5.763
$Al(NO_3)_3$	2.998	$NdCl_3$	5.665
$In(NO_3)_3$	2.834	$ErCl_3$	6.131
$CuCl_2$	2.387	$Yb(NO_3)_3$	4.83
$Cu(NO_3)_2$	3.453	$Eu(NO_3)_3$	5.197
$CuSO_4$	3.821	$Nd(NO_3)_3$	5.044
$Cu(CH_3CO_2)_2$	5.452	$Dy(NO_3)_3$	5.035
NaCl	6.699	$Tm(NO_3)_3$	5.976
KCl	6.578	$Gd(NO_3)_3$	5.017
LiCl	6.768	$Pr(NO_3)_3$	4.704
$CaCl_2$	5.462	$La(NO_3)_3$	4.682
$ZnCl_2$	5.872	$Ce(NO_3)_3$	4.764
$BaCl_2$	6.489	$Tb(NO_3)_3$	4.534
$NiCl_2$	5.334	$Ho(NO_3)_3$	6.038
$MgCl_2$	5.511	$Sm(NO_3)_3$	4.505
$SmCl_3$	5.380	$Y(NO_3)_3$	4.509
YCl_3	6.346	$Lu(NO_3)_3$	5.228
$NdCl_3$	5.665	$Er(NO_3)_3$	5.290

[a] The concentration of the solution is 25 mM. pH values were measured by a METTLER TOLEDO (S479-uMix) pH meter.

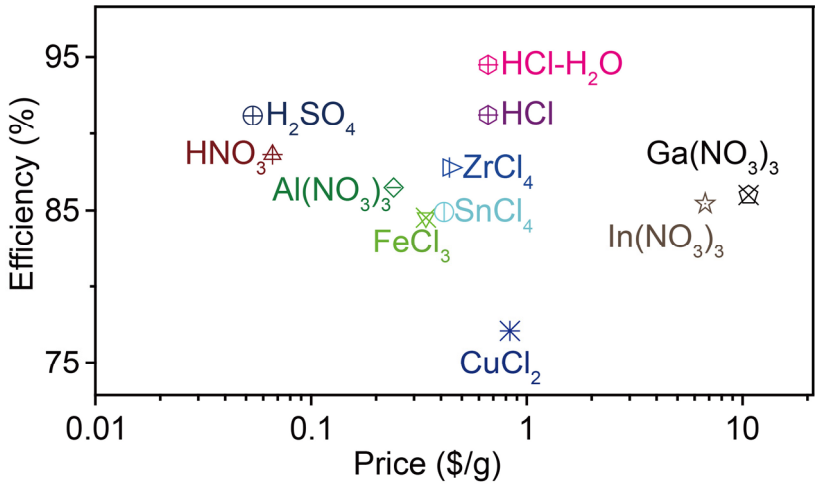

Figure S9. Oleate ligand-removal efficiencies by using different reagents and corresponding prices of the reagents. HCl-H_2O represents the commonly used HCl washing method. The prices were calculated according to the prices presented in the Sigma-Aldrich website. Note that ligand-removal efficiency was calculated based on the TG analysis by the following equation:

$$Efficiency\ (\%) = 100 - \frac{losed\ weight\ of\ treated\ UCNPs\ in\ 280 - 600\ ℃}{losed\ weight\ of\ ligand - capped\ UCNPs\ in\ 280 - 600\ ℃}$$

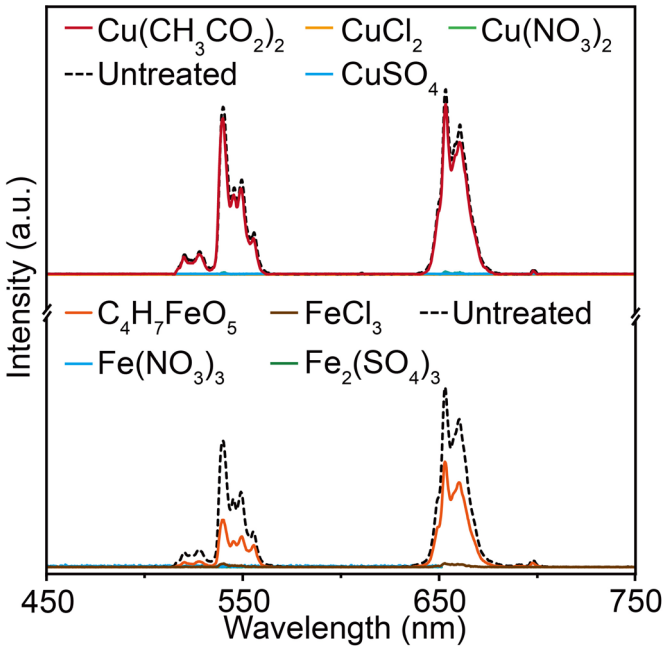

Figure S10. Upconversion luminescence spectra of the cyclohexane layer after shaking the mixture of the oleate ligand-capped UCNPs in cyclohexane and a selected metal salt in DMF for ~10 s. The disappearance of upconversion luminescence in the cyclohexane layer reveals the removal of oleate ligands from UCNPs and the transfer of UCNPs to DMF.

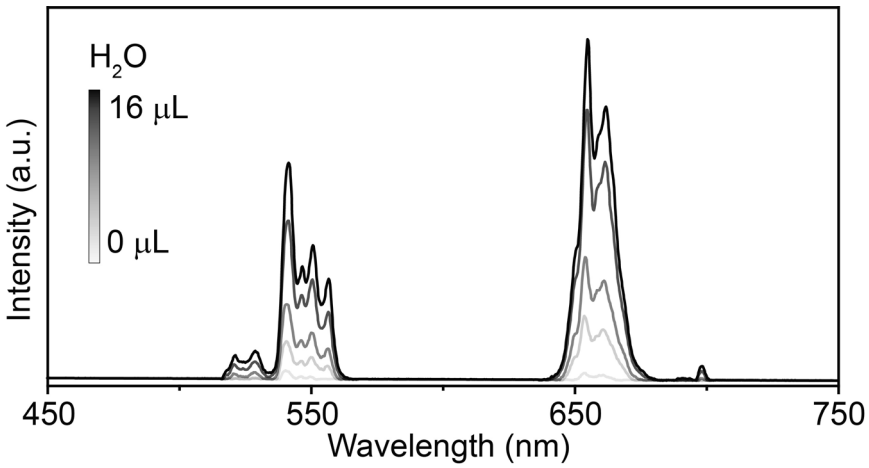

Figure S11. Upconversion luminescence spectra of the DMF layer after the addition of varied amounts of water to superdry DMF containing $FeCl_3$. The spectra were recorded after shaking the mixture of the oleate ligand-capped UCNPs in cyclohexane and $FeCl_3$ in DMF for ~10 s.

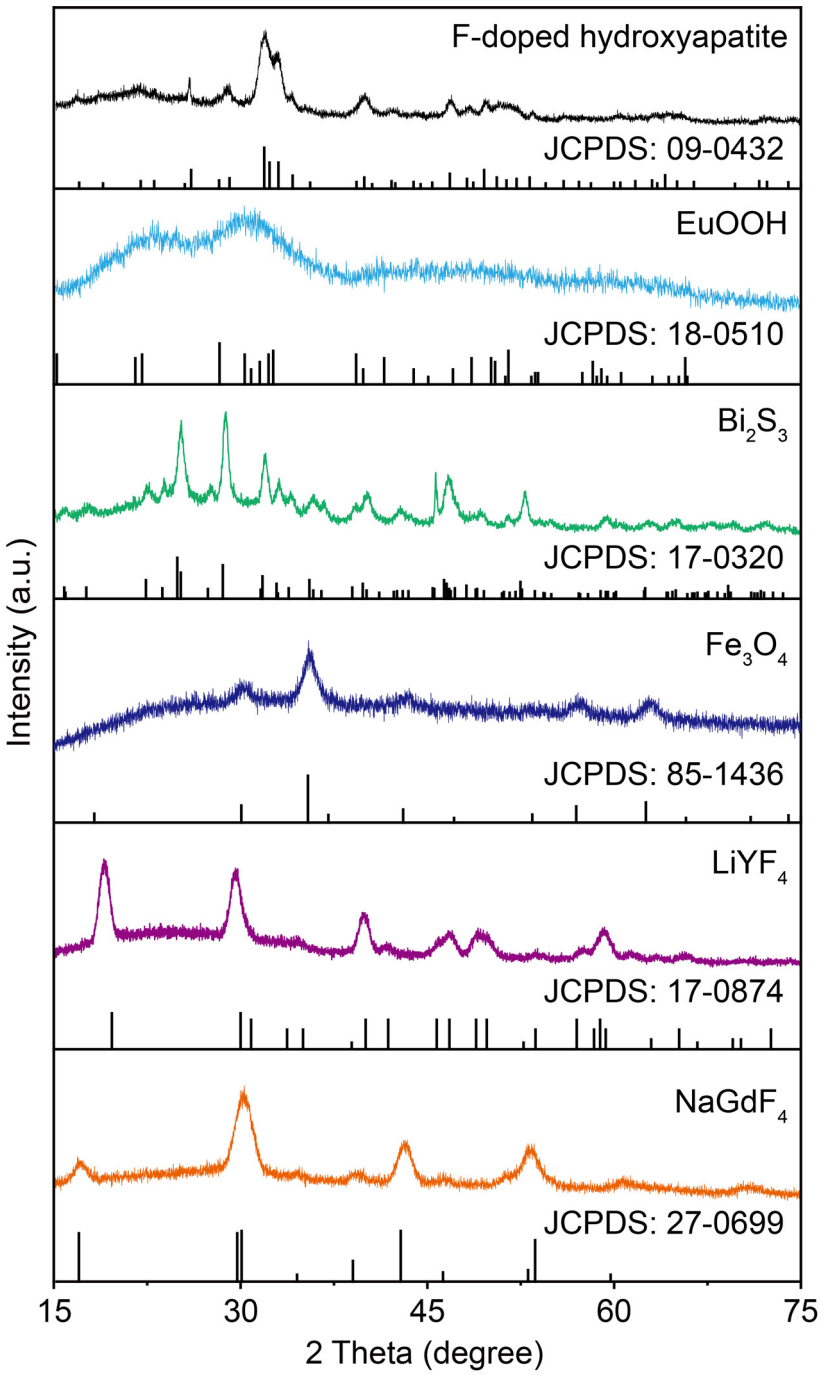

Figure S12. XRD patterns of ligand-capped F-doped hydroxyapatite (F-doped $Ca_5(OH)(PO_4)_3$), EuOOH, Bi_2S_3, Fe_3O_4, $LiYF_4$:Yb/Tm (20/1 mol%), and $NaGdF_4$:Yb/Tm (49/1 mol%) nanomaterials. The diffraction patterns at the bottom of each measured pattern are the literature references for the $Ca_5(OH)(PO_4)_3$ (JCPDS: 09-0432), EuOOH (JCPDS: 18-0510), Bi_2S_3 (JCPDS: 17-0320), Fe_3O_4 (JCPDS: 85-1436), tetragonal $LiYF_4$ (JCPDS: 17-0874), and hexagonal $NaGdF_4$ (JCPDS: 27-0699) crystals, respectively. Notably, due to the small size of as-synthesized EuOOH nanowires, only broad peaks can be observed in the XRD pattern.[2] For $NaGdF_4$:Yb/Tm UCNPs, certain peaks (e.g., peaks at ~52 and 55°), which are not listed in the literature reference can still be ascribed to hexagonal $NaGdF_4$ crystals according to previous reports of other hexagonal $NaLnF_4$ (Ln = Y, Eu, Ho, and Tb) nanomaterials.

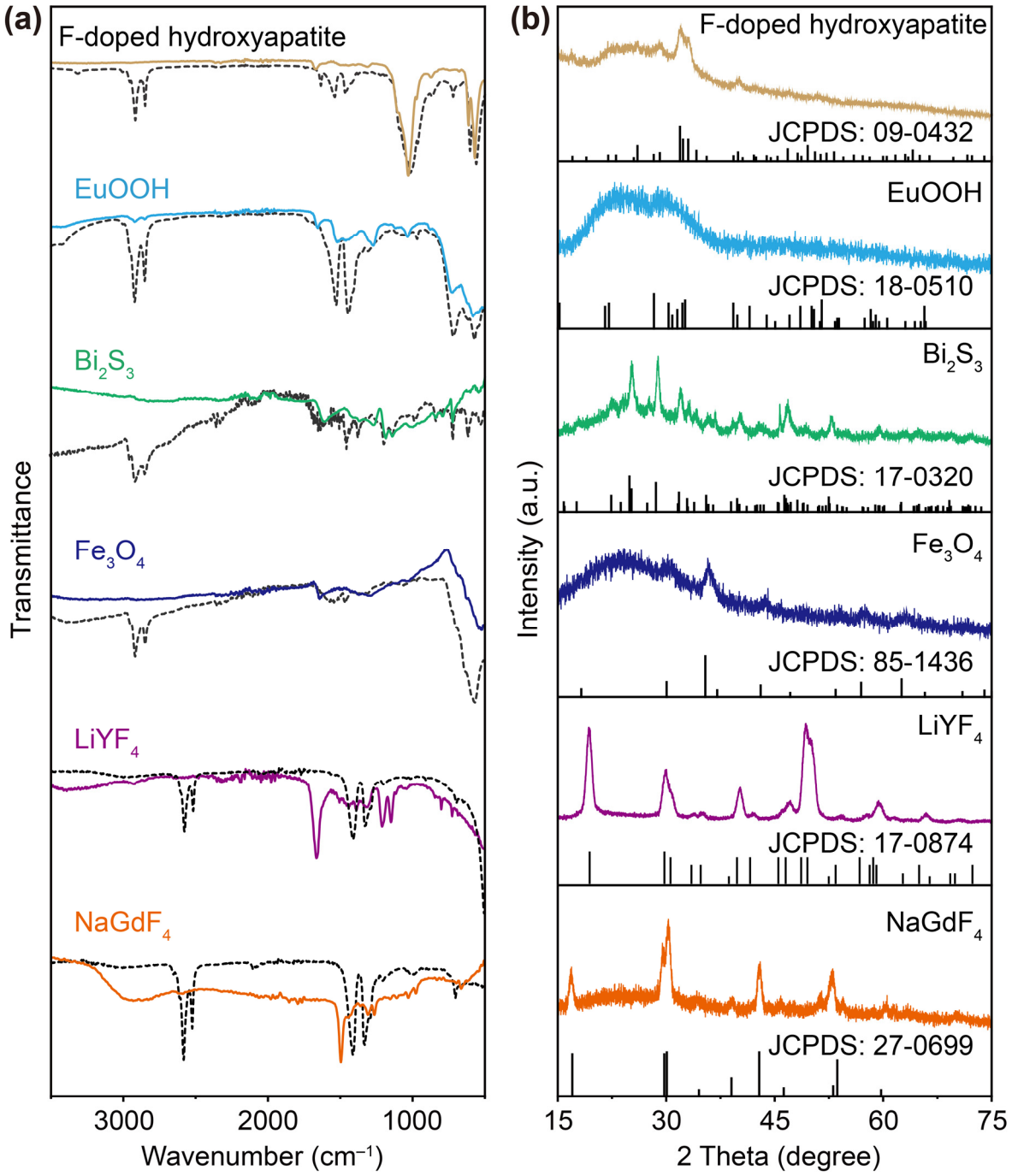

Figure S13. (a) FT-IR spectra and (b) XRD patterns of F-doped hydroxyapatite (F-doped $Ca_5(OH)(PO_4)_3$), EuOOH, Bi_2S_3, Fe_3O_4, $LiYF_4$:Yb/Tm (20/1 mol%), and $NaGdF_4$:Yb/Tm (49/1 mol%) nanomaterials after the treatment of $Al(NO_3)_3$. The black dashed lines in (a) are the FT-IR spectra of corresponding ligand-capped nanomaterials. The diffraction patterns at the bottom of each measured pattern in (b) are the literature references for the $Ca_5(OH)(PO_4)_3$ (JCPDS: 09-0432), EuOOH (JCPDS: 18-0510), Bi_2S_3 (JCPDS: 17-0320), Fe_3O_4 (JCPDS: 85-1436), tetragonal $LiYF_4$ (JCPDS: 17-0874), and hexagonal $NaGdF_4$ (JCPDS: 27-0699) crystals, respectively.

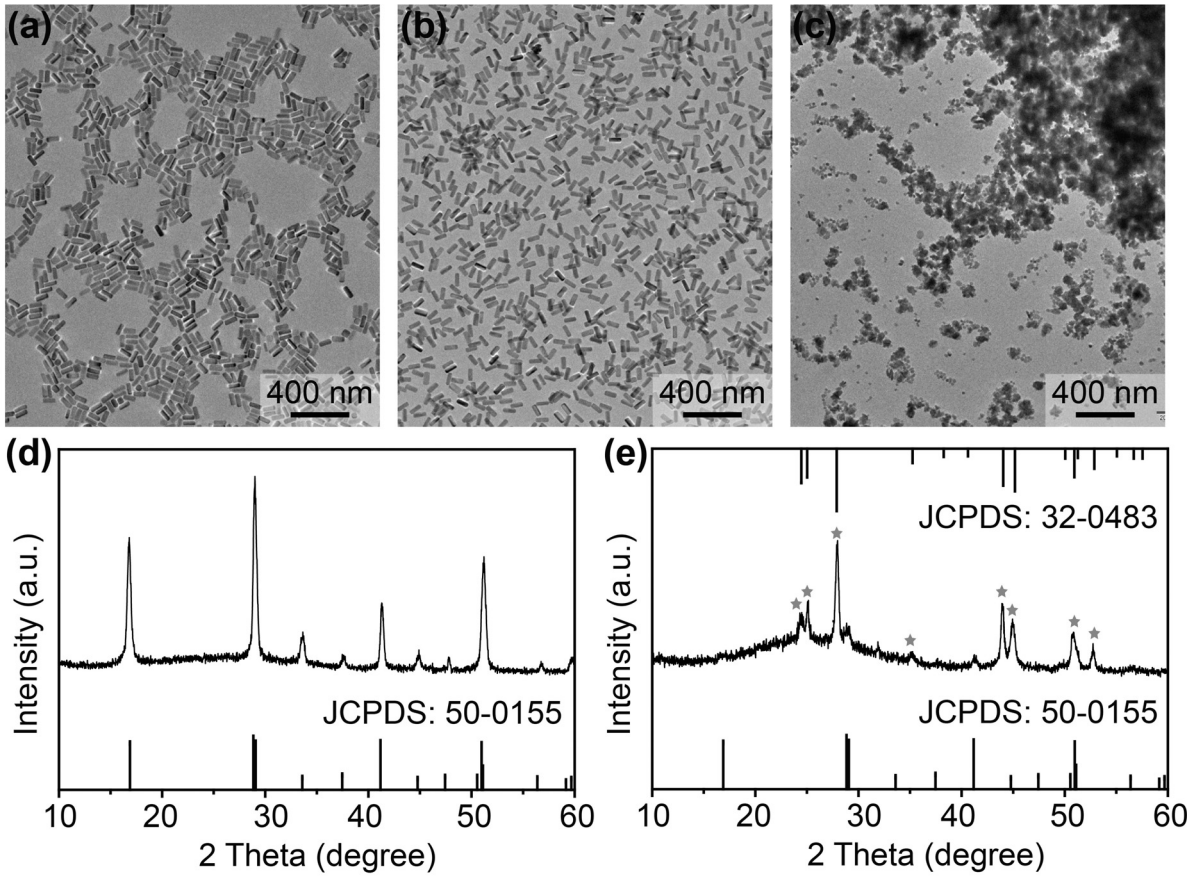

Figure S14. (a) TEM image of ligand-capped $NaLaF_4$ nanoparticles. (b, c) TEM images of corresponding $NaLaF_4$ nanoparticles shown in (a) after treated by (b) our strategy and (c) HCl washing method. (d, e) XRD patterns of the treated $NaLaF_4$ nanoparticles shown in (b) and (c), respectively. The diffraction patterns at the bottom of (d, e) and on top of (e) are the literature references for the hexagonal $NaLaF_4$ (JCPDS: 50-0155) and LaF_3 (JCPDS: 32-0483) crystals, respectively. Diffraction peaks ascribed to LaF_3 are marked by stars in (e).

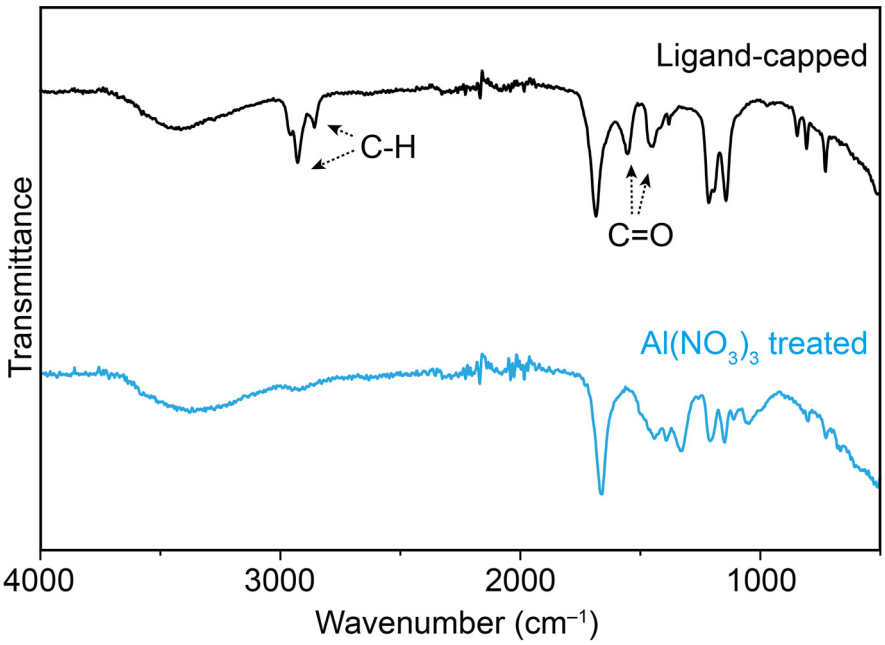

Figure S15. FT-IR spectra of ligand-capped and $Al(NO_3)_3$ treated $NaLaF_4$ nanoparticles. Characteristic peaks of C-H bond (~2923 and 2852 cm^{-1}) and C=O bond (~1560 and 1466 cm^{-1}) arising from oleate ligands are indicated by arrows. After the $Al(NO_3)_3$ treatment, characteristic peaks of oleate ligands almost vanish, indicating the removal of ligands.

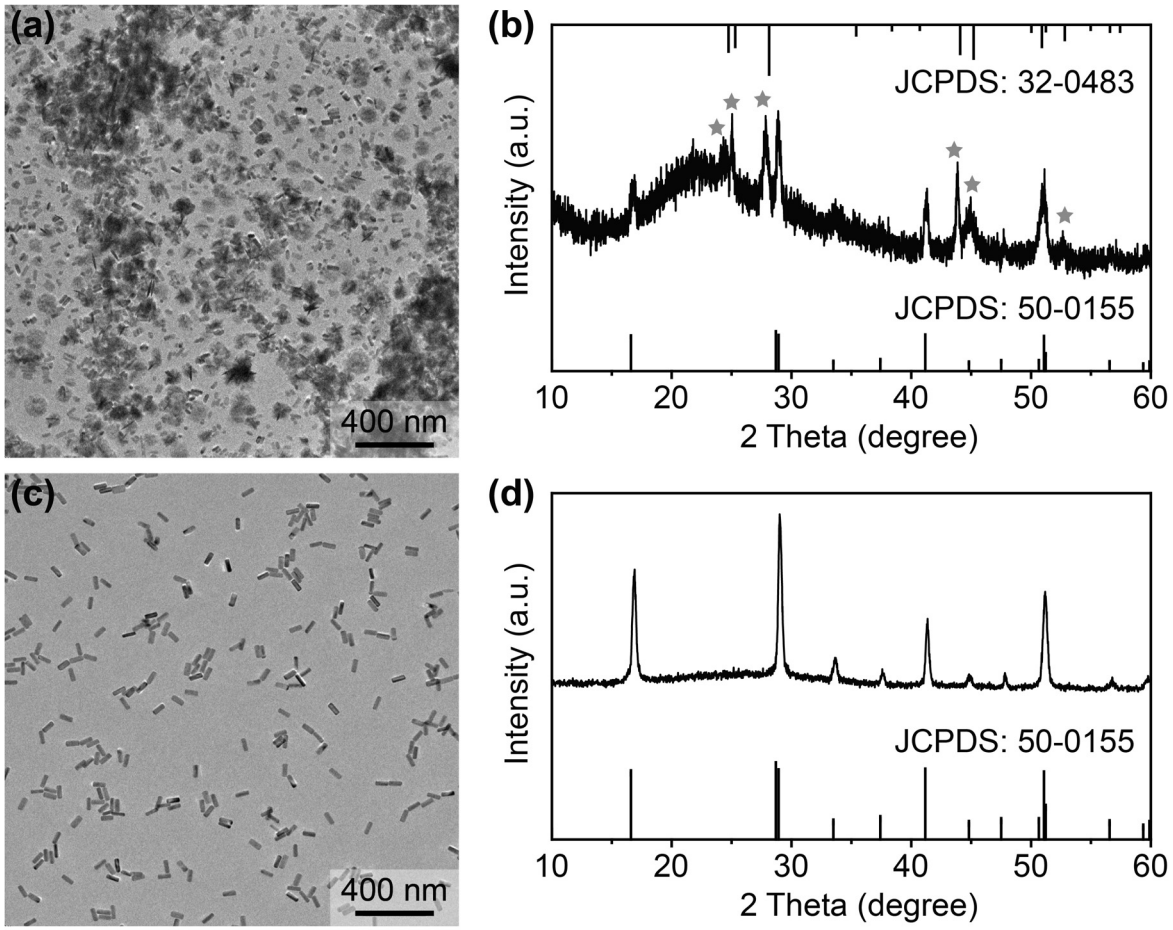

Figure S16. (a) TEM image and (b) corresponding XRD pattern of ligand-capped $NaLaF_4$ nanoparticles after the treatment of HCl washing (HCl, 0.1 M). The diffraction patterns on top and at the bottom of (b) are the literature references for the LaF_3 (JCPDS: 32-0483) and hexagonal $NaLaF_4$ (JCPDS: 50-0155) crystals, respectively. Diffraction peaks ascribed to LaF_3 are marked by stars in (b). (c) TEM image and (d) corresponding XRD pattern of ligand-capped $NaLaF_4$ nanoparticles after the treatment of our strategy using HCl (0.1 M) in DMF as the proton generator. The diffraction pattern at the bottom of (d) is the literature reference for the hexagonal $NaLaF_4$ (JCPDS: 50-0155) crystal.

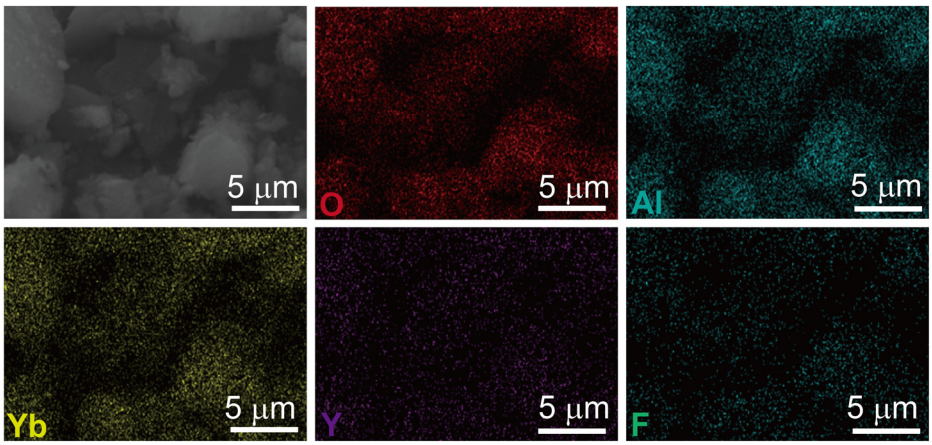

Figure S17. SEM image and corresponding elemental mapping of the as-synthesized UCNP-MIL-100(Al) composite gel.

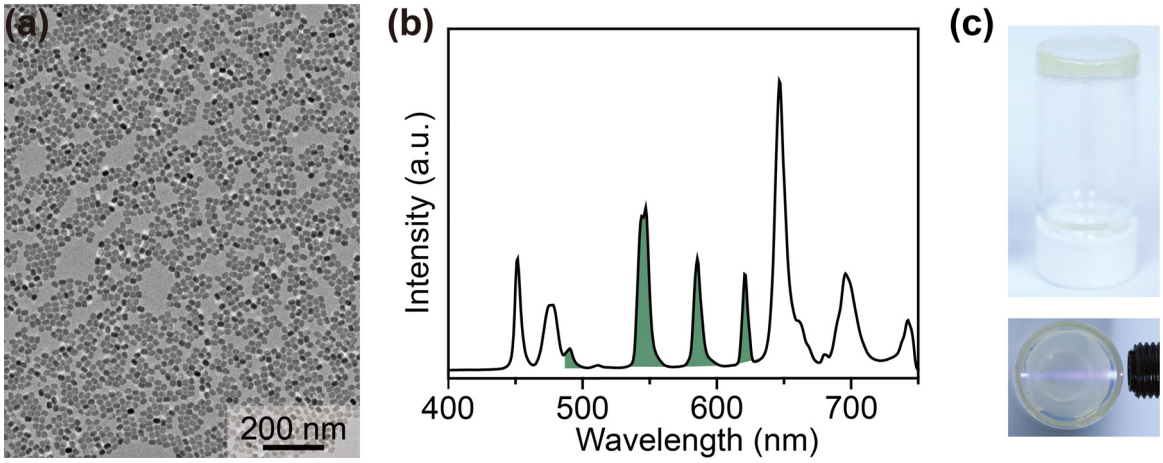

Figure S18. (a) TEM image and (b) upconversion luminescence spectrum of ligand-capped $NaGdF_4$:Yb/Tm (49/1 mol%)@$NaGdF_4$:Tb (15 mol%) UCNPs. The nanoparticles were dispersed in cyclohexane for measuring the spectrum, and upconversion emission of Tb^{3+} is highlighted in the spectrum. (c) Photos showing the UCNP-MIL-100(Al) composite gel, fabricated using UCNPs shown in (a), in daylight (upper panel) and under 980 nm excitation (lower panel).

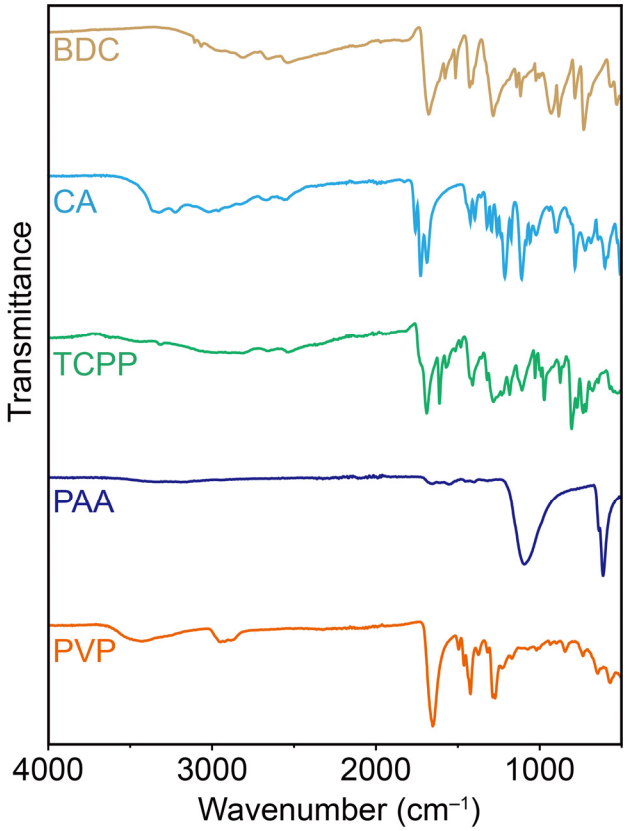

Figure S19. FT-IR spectra of 1,4-benzenedicarboxylic acid (BDC), citric acid (CA), tetrakis(4-carboxyphenyl) porphyrin (TCPP), polyacrylic acid (PAA), and polyvinylpyrrolidone (PVP), respectively.

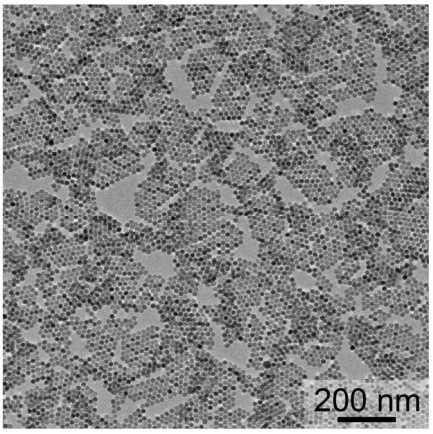

Figure S20. TEM image of the as-synthesized $NaGdF_4$:Yb/Tm (49/1 mol%)@$NaGdF_4$ UCNPs.

3. References

1. J. Hui and X. Wang, *Chem. Eur. J.*, 2011, **17**, 6926–6930.
2. S. Zhang, W. Shi, S. Rong, S. Li, J. Zhuang and X. Wang, *J. Am. Chem. Soc.*, 2020, **142**, 1375–1381.
3. R. Malakooti, L. Cademartiri, Y. Akçakir, S. Petrov, A. Migliori and G. Ozin, *Adv. Mater.*, 2006, **18**, 2189–2194.
4. J. Park, K. An, Y. Hwang, J. Park, H. Noh, J. Kim, J. Park, N. Hwang and T. Hyeon, *Nat. Mater.*, 2004, **3**, 891–895.
5. C. Lin, Z. Xia, L. Zhang, X. Chen, Q. Sun, M. Lu, Z. Yuan, X. Xie and L. Huang, *ACS Appl. Mater. Interfaces*, 2020, **12**, 31783−31792.